Supporting Information

Tetrazole substituted polymers for High Temperature Polymer Electrolyte Fuel Cells

Dirk Henkensmeier,[a,b]* Ngoc My Hanh Duong,[a,b] Mateusz Brela,[c] Karol Dyduch,[c] Artur Michalak,[c]* Katja Jankova,[d] Hyeongrae Cho,[a] Jong Hyun Jang,[a,e] Hyoung-Juhn Kim,[a] Lars N. Cleemann,[d] Qingfeng Li,[d] Jens Oluf Jensen[d]

a) Korea Institute of Science and Technology, Fuel Cell Research Center, Hwarangno 14-gil 5, 136-791 Seoul, Republic of Korea

b) University of Science and Technology, 217 Gajungro, Yuseonggu, Daejeon, Republic of Korea

c) Jagiellonian University, Faculty of Chemistry, Ingardena 3, 30-060 Krakow, Poland

d) Proton Conductors, DTU Energy, Technical University of Denmark, Kemitorvet 207, DK-2800 Kgs. Lyngby, Denmark

e) Green School, Korea University, Seoul 136-713, Republic of Korea

* corresponding authors: henkensmeier@kist.re.kr; michalak@chemia.uj.edu.pl.

*Synthesis of **P1***

1.394 g (10 mmol) 2,6-difluorobenzonitrile, 2.2829 g (10 mmol) bisphenol A and 4 g potassium carbonate (K_2CO_3) were dissolved in a mixture of 25 ml anhydrous NMP and 50 ml toluene. After thorough flushing with argon, the mixture was heated under reflux for 4 hours to remove water by azeotropic distillation with toluene (Dean-Stark-trap), and after removal of toluene ca. 18 hours more at 145 °C. The reaction mixture was cooled down, the polymer precipitated in DI water, washed several times with water and methanol, and dried under reduced pressure at 60 ºC. Yield: 2.87 g. ^{1}H NMR (300 MHz, DMSO-d6, ppm): 7.52 (m, 1H, proton *para* to nitrile), 7.34 (m, 4H, protons *meta* to isopropylidene), 7.14 (m, 4H, protons *ortho* to isopropylidene), 6.59/6.60 (m, 2H, proton *meta* to nitrile), 1.70 (s, 6H, isopropylidene).

Synthesis of **P2**

1.9627 g (10 mmol) hydroquinone sulfonic acid potassium salt (HQSA) and 4 g potassium carbonate (K$_2$CO$_3$) were dissolved in a mixture of 30 ml DMAc and 40 ml toluene. After thorough flushing with argon, the mixture was heated under reflux to remove the water by azeotropic distillation with toluene (Dean-Stark-trap). After removal of toluene, 1.3911 g (10 mmol) 2,6-difluorobenzonitrile were added and the mixture heated for several hours at 180 °C. The reaction mixture (which is not very viscous) was cooled down, and the polymer precipitated in DI water and separated from the solution by filtration or centrifugation. After drying under reduced pressure at 60 °C, 0.79 g polymer were obtained. ^{1}H NMR (300 MHz, DMSO-d6, ppm): 7.61 - 7.25 (m, 4H, proton *para* to nitrile and protons from HQSA), (6.91/6.93), 6.77/6.79, 6.63/6.65, 6.48/6.51 and 6.39/6.41(m, 2H, protons *meta* to nitrile).
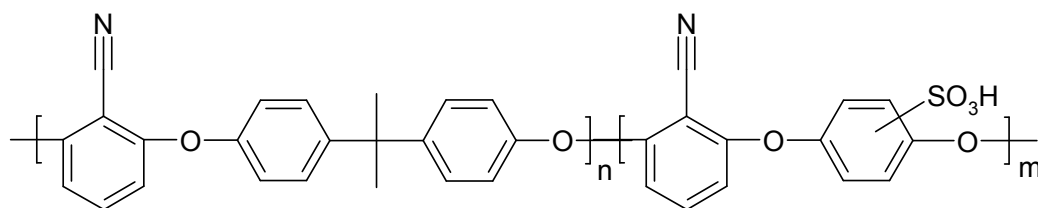
SPEEN, n:m = 6:4
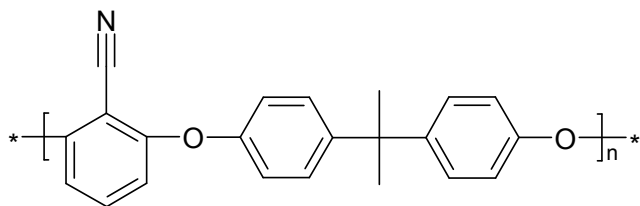
P1
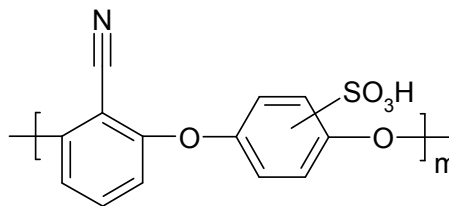
P2

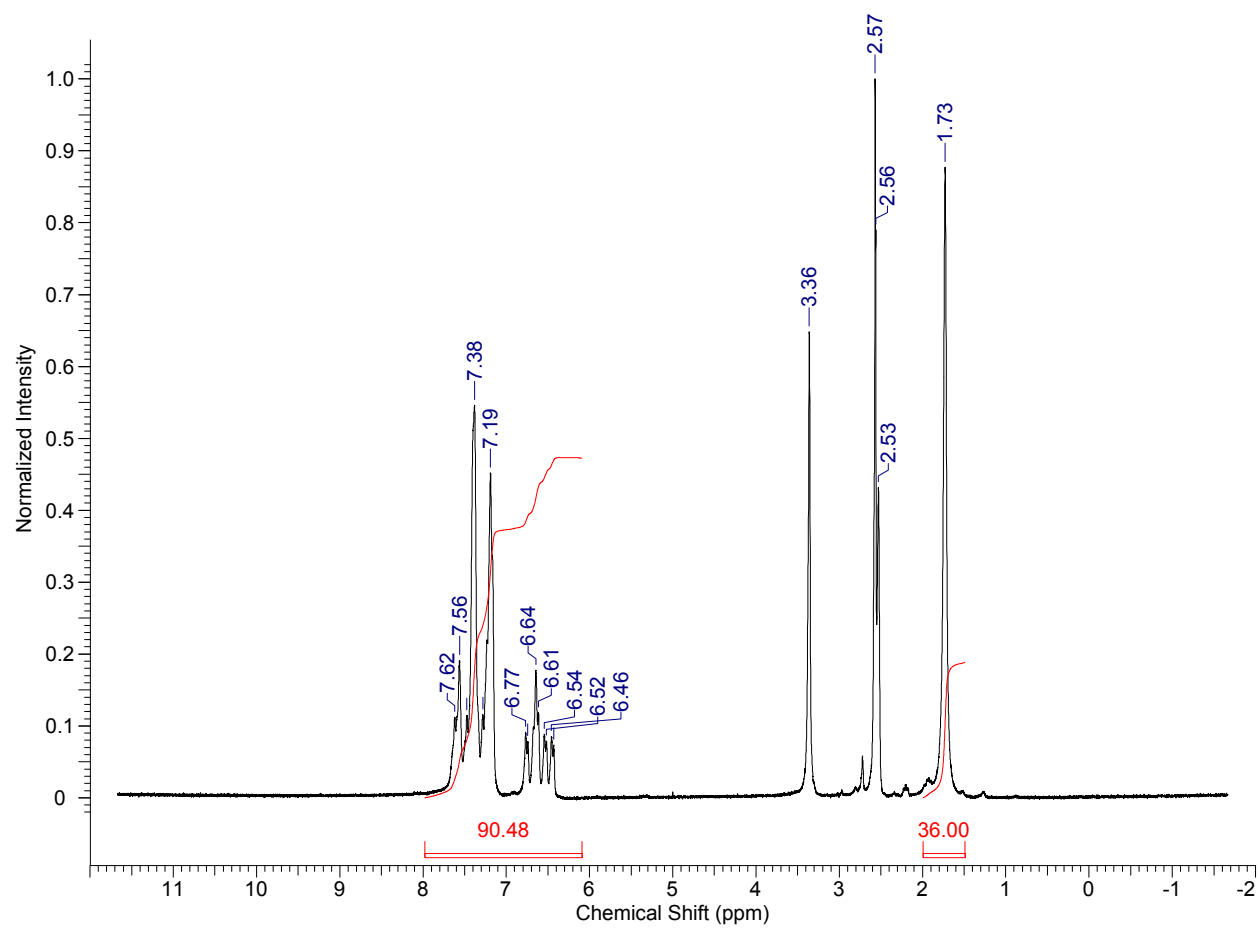**Figure S1**: Structures of SPEEN, P1 and P2.
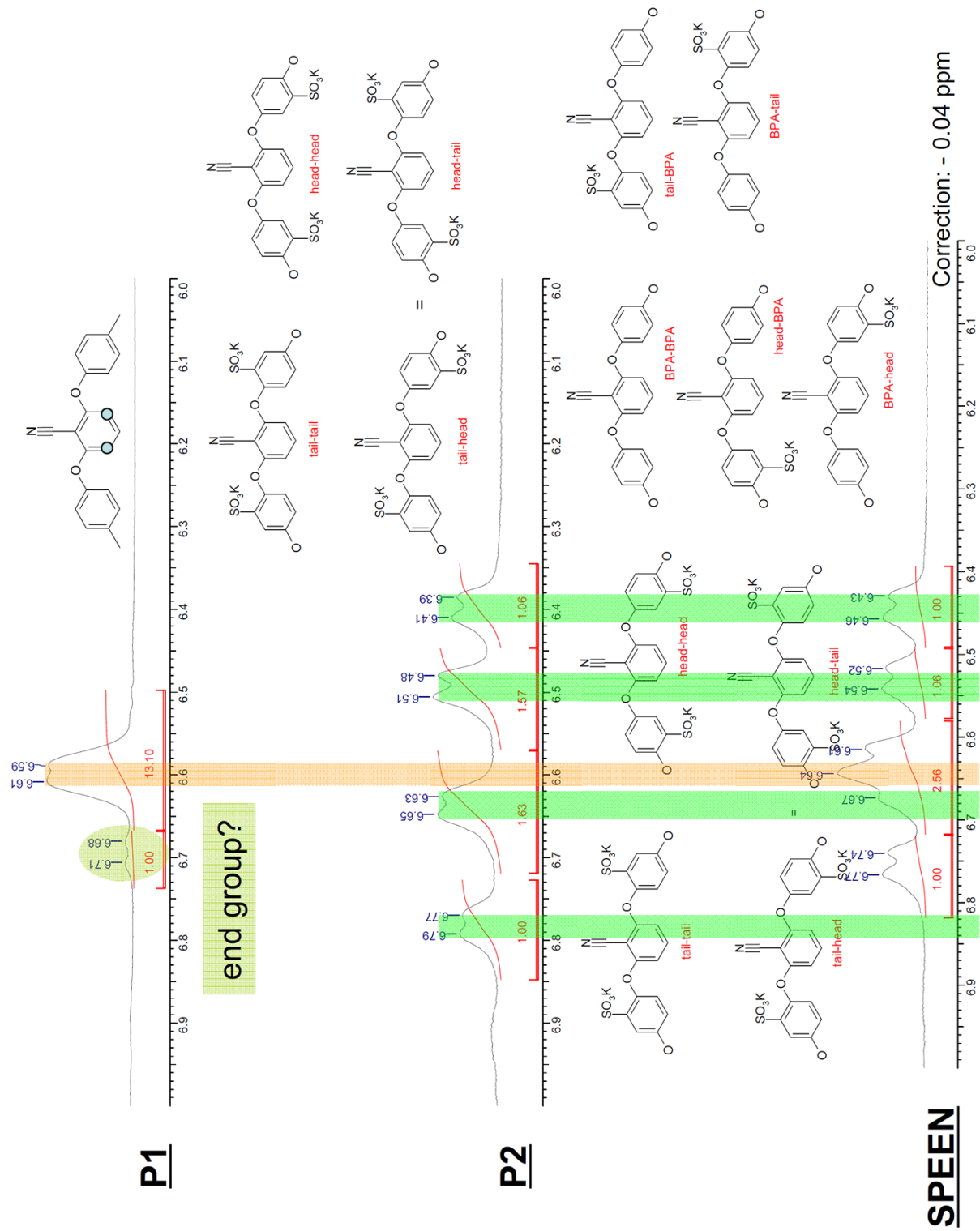
Figure S2: NMR spectrum of SPEEN.

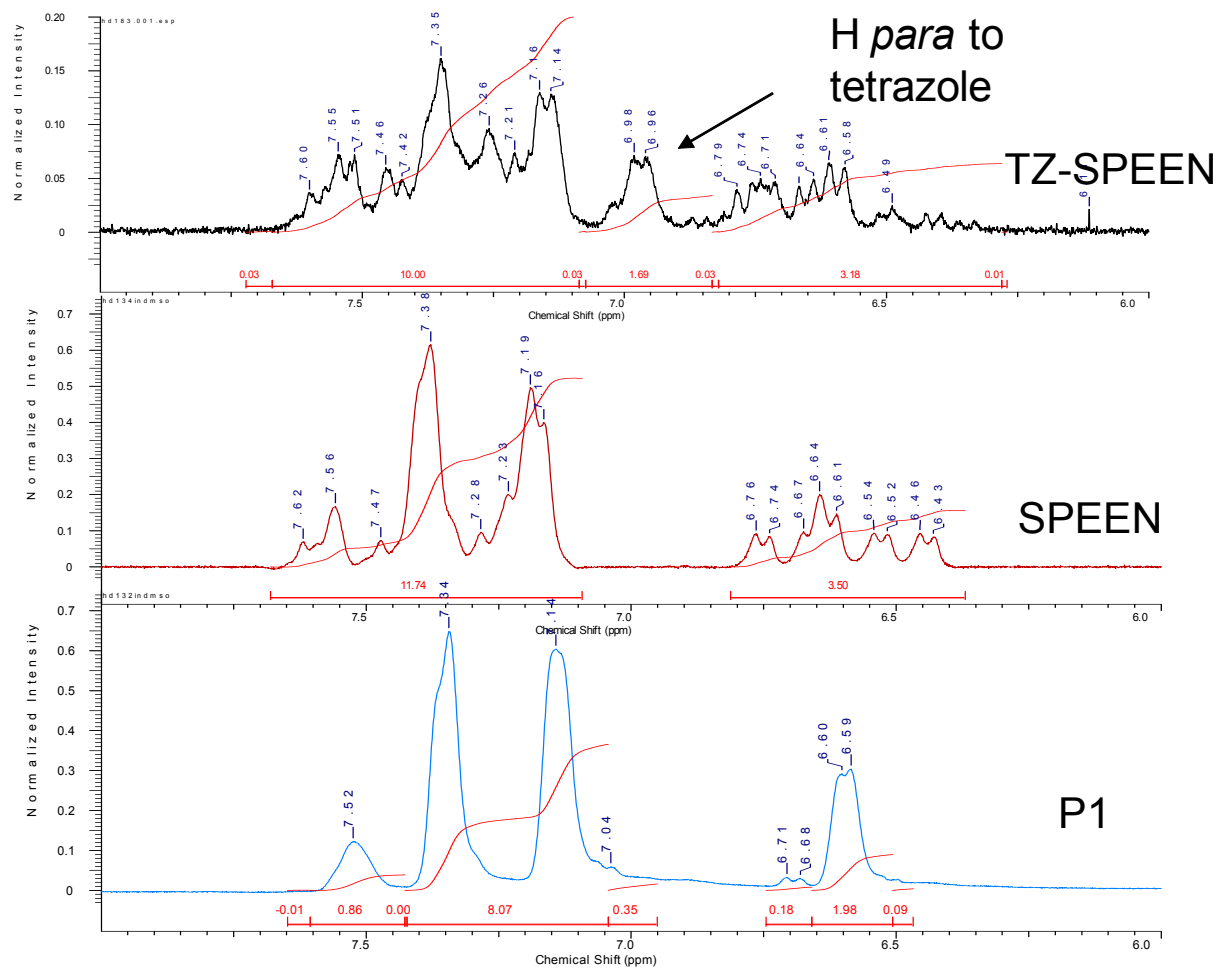**Figure S3**: NMR spectra of SPEEN, P1 and P2.

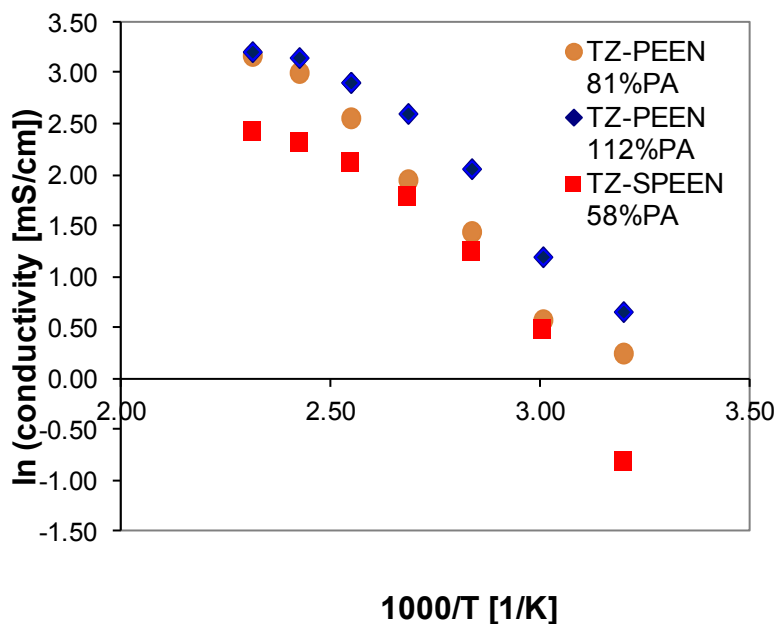**Figure S4**: NMR spectra of TZ-SPEEN, SPEEN and P2.

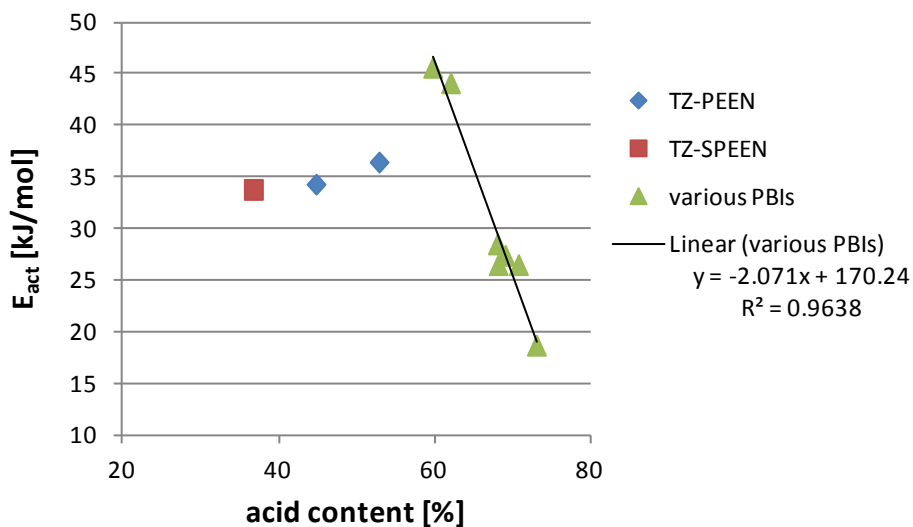**Figure S5**: Arrhenius plot of PA doped TZPEEN and TZ-SPEEN membranes.

Figure S6: Comparison of the proton conduction activation energy of TZ-PEEN and TZ-SPEEN (obtained from the linear regions in Figure S5), and data from Asensio et al.
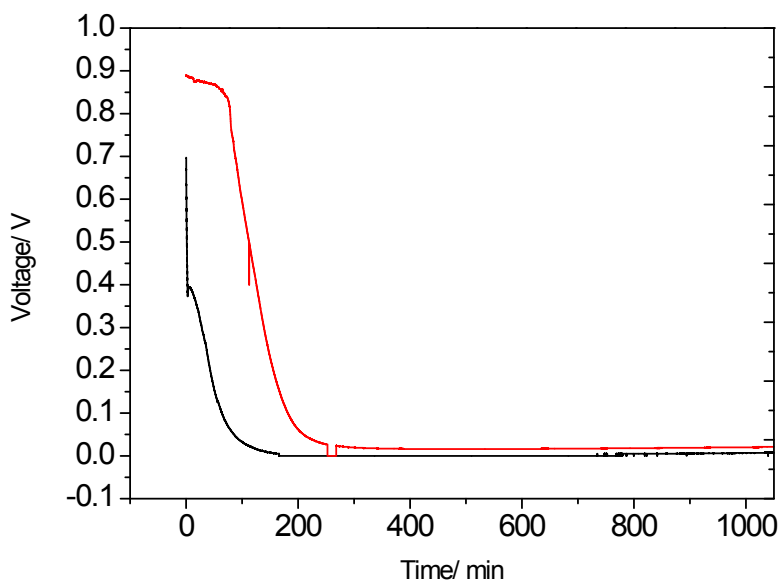
Figure S7: Development of the potential at 0.2 A.cm^{-2} with time for a 40 μm thick TZ-SPEEN membrane (**MEA1**), doped to a PA uptake of 56% (not dried). Red curve: degradation of potential after the operating temperature of 160 °C was reached. Black curve: potential after shut-down and start-up.

After shut-down and re-start of the cell, the potential partially recovered but dropped again rapidly (black curve). At the end of test, an iV curve was measured. The extremely low OCV clearly indicated that the cell failed due to pinhole or crack formation. After the FC test the TZ-PEEN membrane was washed free from PA and immersed in DMAc/LiCl for SEC analysis. Apparently the membrane was partially crosslinked, and SEC analysis of the ca. 10 wt.-% soluble fraction showed that the polymer was degraded. The SEC curve of the soluble fraction was almost completely shifted to low molar masses with Mn of 6,800 and Mw of 15,600 (**Figure S9**). Due to the disappearance of the high MW fraction the PDI decreased from 3,48 to 2,29
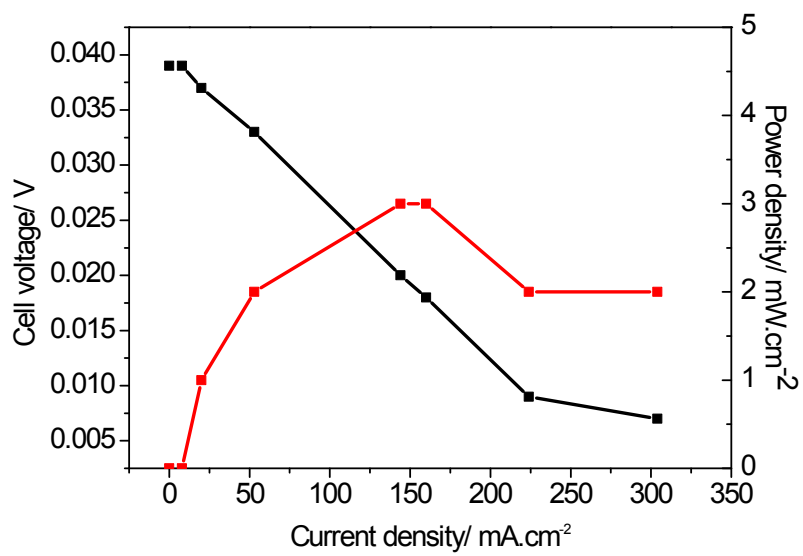
Figure S8: Polarization curve and power density curve of a 40 μm thick PA doped TZ-SPEEN membrane (**MEA1**).

Figure S9: SEC curves of TZ-SPEEN before (1) and after the fuel cell test (2).

Figure S10: Linear sweep voltammetry of **MEA2**, a 52 μm thick TZ-PEEN membrane, doped to a PA uptake of 46% PA (wet), after 24 hours operation; cell temperature 160 °C.

References:

J. A. Asensio, E. M. Sánchez, P. Gómez-Romero, *Chem. Soc. Rev.* **2010**, *39*, 3210–3239.

Preliminary theoretical results for larger models involving multiple protonation

The main goal of the theoretical analysis presented in the manuscript was to compare:

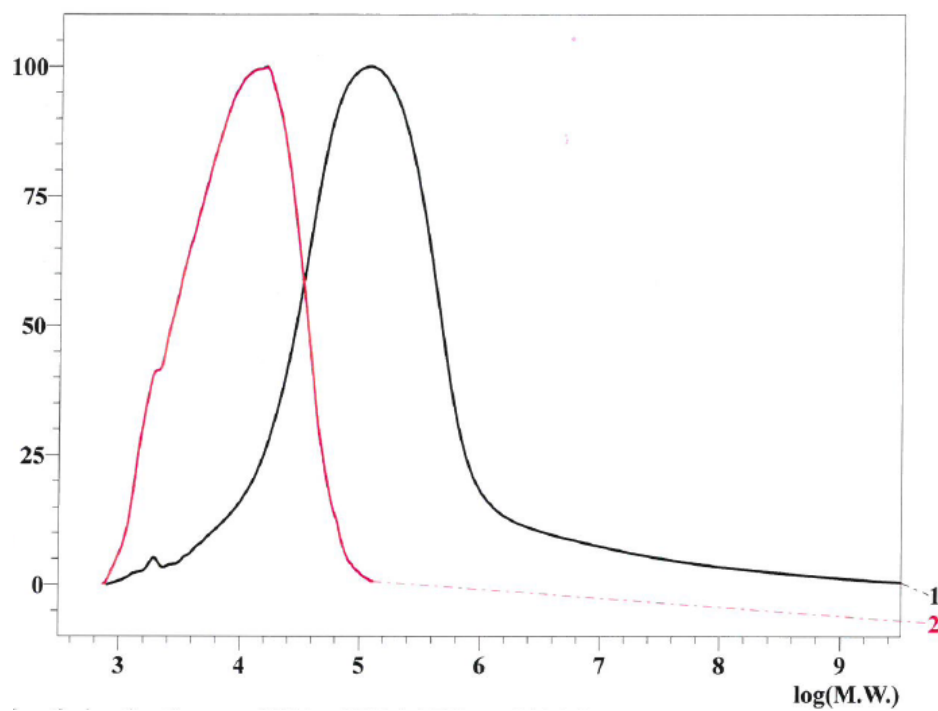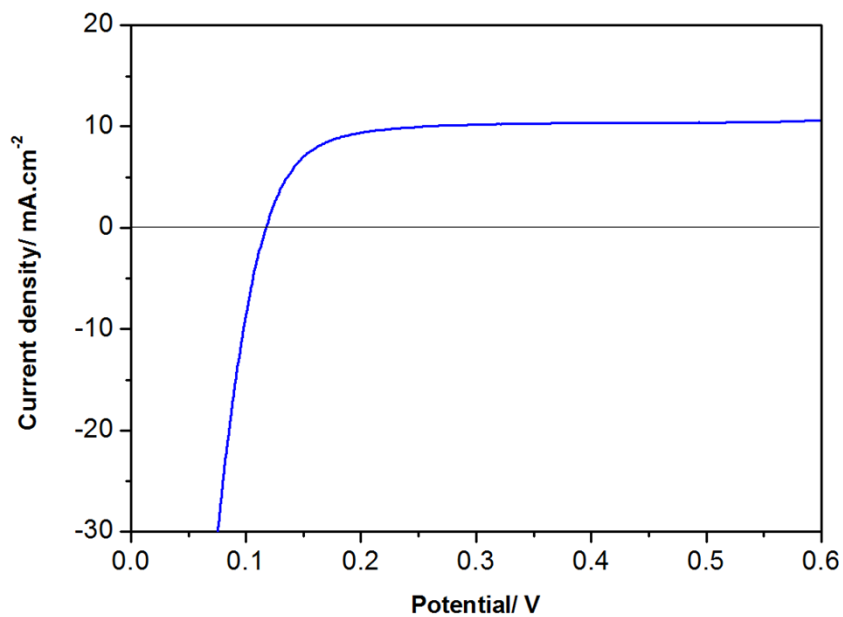1)   protonation of simple tetrazole and benzimidazole molecules;

2)   the effect of the aryl-ether group in TZPEEN 'monomer', and the phenyl group in PBI 'monomer' on the protonation;

3)   the effect of the neighbouring units especially in the TZ based trimer.

The main conclusions are:

   (i)   there is a quite large difference of ca. 27 kcal/mol in the protonation energies of free tetrazole and benzimidazole;

   (ii)   in the 'monomers' and 'trimers' this difference practically disappears, due to extra stabilization in TZPEEN coming from the ether oxygens (which is explained by the electrostatic potential maps).

However, it is important to emphasize that relatively small polymer models were used, and only the single protonation of the central unit was considered. Also, in the real system, multiple protonation of the polymer chain should be facile. Obviously, the protonation energies will be affected by the number and position of already protonated units. Therefore, it is important to validate how much the picture can change when longer polymer models are considered for single protonation, as well as when multiple protonation is considered.

The main goal of the preliminary calculations presented here was to verify, if the *qualitative* picture changes (concerning comparison of tetrazole and PBI) when the factors mentioned above are considered.

Effect of the polymer model on the single protonation of TZ-PEEN and PBI

In order to validate our main conclusion for larger models, the preliminary calculations were performed for the tetrazole model comprising four repeat units ('tetramer', **1d**), and for PBI models with four and six benzimidazole fragments ('dimer' and 'trimer', **2d** and **2e**, respectively), see **Figure S11**. The geometries of these systems were built based on the previously optimized structures, and re-optimized. The results presented in **Table S1** show that that there is no qualitative influence of the model elongation, concerning the trends in the protonation energies for the tetrazole- and PBI-based systems.

Table S1. The protonation energies, $\Delta E_{p,1}$ in kcal/mol. The structures are shown in **Figure S11**.

Systems:		$\Delta E_p{}^1$
Tetrazole	**1a** + H$^+$ → **1a-H$^+$**	-206.43 (-37.59)
TZ-PEEN 'monomer'	**1b** + H$^+$ → **1b-H$^+$**	-240.48 (-71.64)
TZ-PEEN 'trimer'	**1c** + H$^+$ → **1c-H$^+$**	-245.53 (-76.69)
TZ-PEEN 'tetramer'	**1d** + H$^+$ → **1d-H$^+$**	-239.13 (-70.29)
Benzimidazole	**2a** + H$^+$ → **2a-H$^+$**	-233.78 (-64.94)
Ph-BI (PBI 'half-mer')	**2b** + H$^+$ → **2b-H$^+$**	-240.37 (-71.53)
PBI 'one and half-mer'	**2c** + H$^+$ → **2c-H$^+$**	-246.73 (-77.89)
PBI 'dimer'	**2d** + H$^+$ → **2d-H$^+$**	-243.18 (-74.34)
PBI 'trimer'	**2e** + H$^+$ → **2e-H$^+$**	-241.27 (-72.43)

[1] reaction energy for X + H$^+$ → XH$^+$ and for X + H$_3$O$^+$ → XH$^+$ + H$_2$O (in brackets)
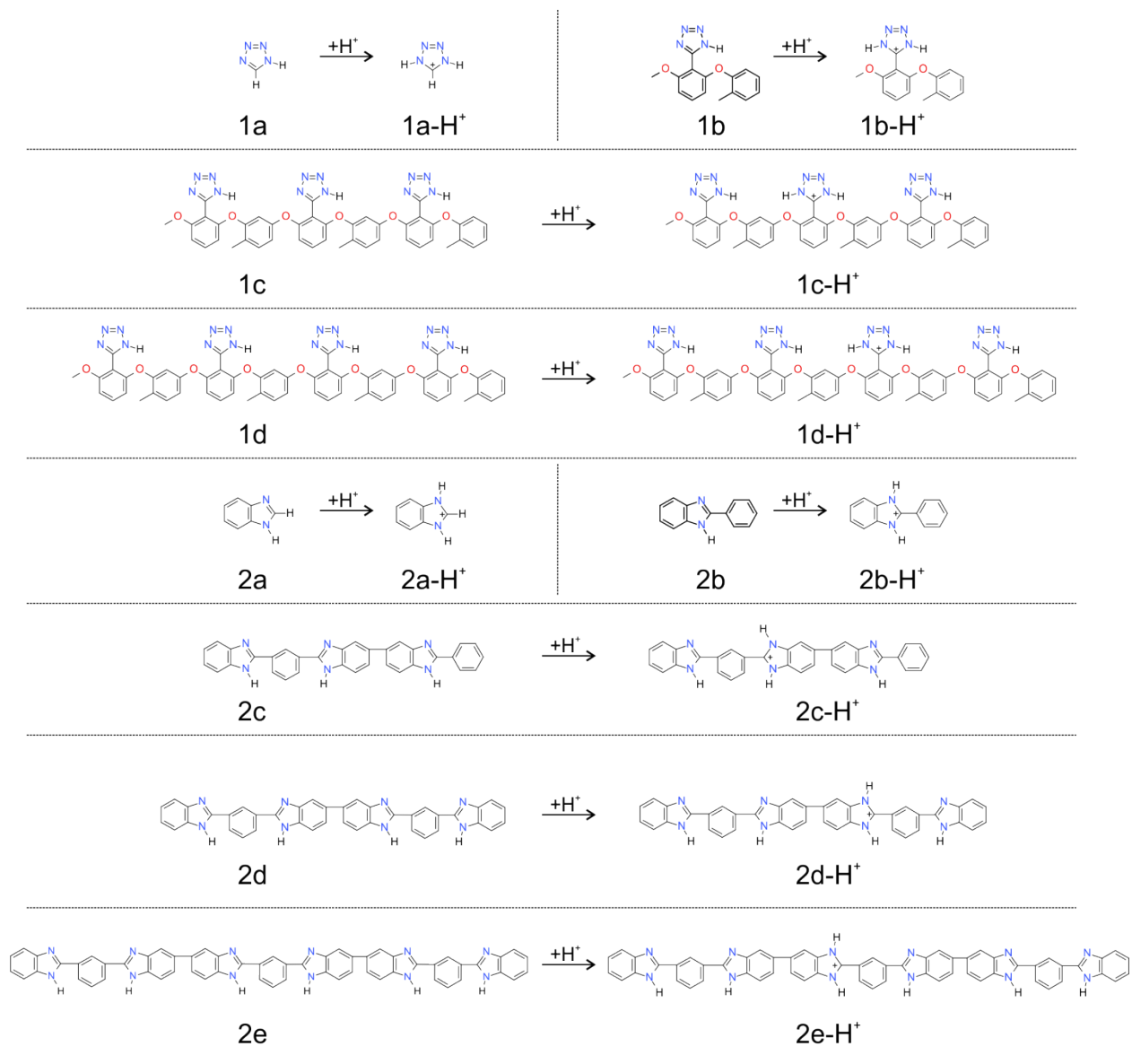
Figure S11. Structures/protonation reactions for the systems considered in **Table S1**.

Double protonation of central and terminal units (neutral systems)

The systems/protonation reactions presented in **Figure S12** were studied to qualitatively investigate the double protonation reactions; the corresponding energies are shown in **Table S2**. The tetrazole 'tetramer', **1d,** and the corresponding PBI 'dimer' (with four protonation sites), **2d,** were considered; further the PBI trimer (containing six possible protonation sites), **2e,** was also included to roughly estimate the effect of the chain length. It should be emphasized that the presence of phosphoric acid (PA) was neglected in the preliminary results for the model reactions considered here. To realistically model the double protonation (involving the protonation of already protonataed polymer chain), PA should be included. Thus, the results presented here should be considered only as a qualitative estimation of the studied effect.

The results presented in two parts of Table S2 show that the values of the protonation energies obviously change, but the qualitative difference between TZ-PEEN and PBI is hardly affected. TZ-tetramer vs. PBI dimer: -445.5 kcal/mol (**1d**) vs. 444.9 kcal/mol (**2d**) for protonation of the central units, and -461.7 kcal/mol (**1d**) vs. -458.8 kcal/mol (**2d**) for protonation of terminal units; the preference for TZPEEN protonation is slightly larger here. The effect of the chain length (2d vs. 2e), although noticeable, is not qualitatively important.

Table S2. The double protonation energies, ΔE_p ,[1] in kcal/mol. The structures are shown in **Figure S12**.

Systems/protonation reactions:		ΔE_p^1
Double Protonation of central units:		
1d: 0000 → 0++0	**1d** + 2H⁺ → **1d-2H⁺**	-445.50 (-107.82)
2d: 0000 → 0++0	**2d** + 2H⁺ → **2d-2H⁺**	-444.86 (-107.18)
2e: 000000 → 00++00	**2e** + 2H⁺ → **2e-2H⁺**	-440.74 (-103.06)
Double Protonation of terminal units:		
1c: 000 → +0+	**1c** + 2H⁺ → **1c-2H⁺**	-461.72 (-124.04)
2c: 000 → +0+	**2c** + 2H⁺ → **2c-2H⁺**	-458.75 (-121,07)

[1] reaction energy for X + 2H⁺ → XH₂²⁺ and for X + 2H₃O⁺ → XH₂²⁺ + 2H₂O (in brackets)
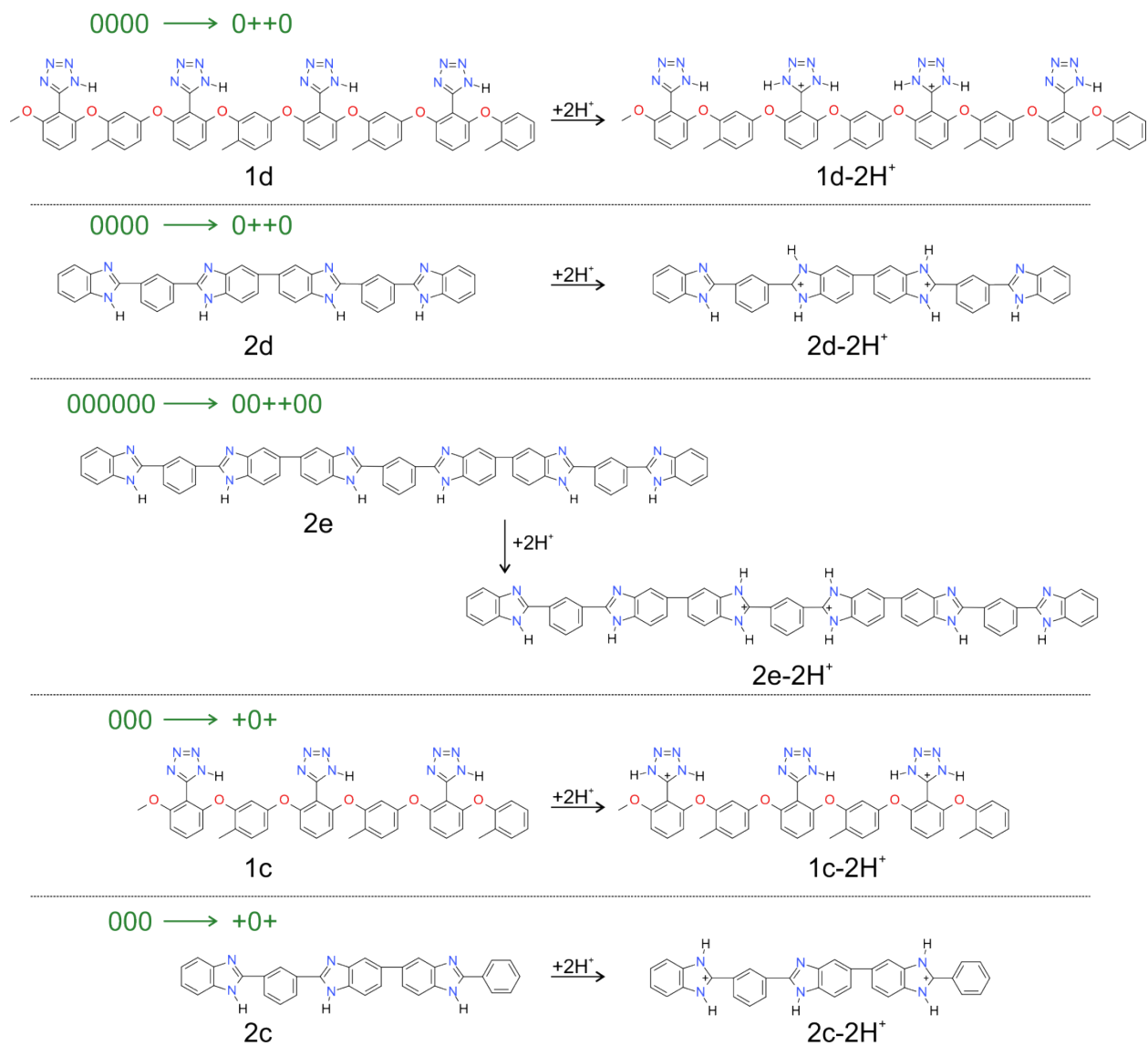
Figure S12. Structures/protonation reactions for the systems considered in **Table S2**.

Effect of protonated-neighbouring units – charged models

Since the electrostatic potential in the resulting, protonated systems is strongly dependent on the total charge of the system, the multiple protonation of the chain cannot be realistically modelled without including the presence of PA anions/molecules in the models. To illustrate this, in **Table S3** we present the calculated protonation energies for the central unit protonation, in the systems with two terminal units already protonated (+0+ → +++), so that the trimer is fully protonated (see **Figure S13**). The results show that the values of the protonation energies are strongly affected, compared to the values of the single protonation in the manuscript (ca. -246 kcal/mol), but the effect is much stronger for PBI than for TZ-PEEN. As the result, the third protonation is now by over 23 kcal/mol more facile for TZ-PEEN than for PBI. It must be strongly emphasized here, however, that the systems considered in **Table S3**, with the high positive charge and complete neglect of anions, represent an unrealistic model. For this reason, we further considered the models with PA species included.

Table S3. The protonation energies for the central unit protonation in the systems with two protonated terminal units (+0+), ΔE_p,[1] in kcal/mol. The structures are shown in **Figure S13**.

Systems/protonation reactions:		ΔE_p^1
1c: +0+ → +++	**1c-2H⁺ + H⁺ → 1c-3H⁺**	-167.19 (1.65)
2c: +0+ → +++	**2c-2H⁺ + H⁺ → 2c-3H⁺**	-145.74 (23.10)

[1] reaction energy for $XH_2^{2+} + H^+ \rightarrow XH_3^{3+}$ and for $XH_2^{2+} + H_3O^+ \rightarrow XH_3^{3+} + H_2O$ (in brackets)
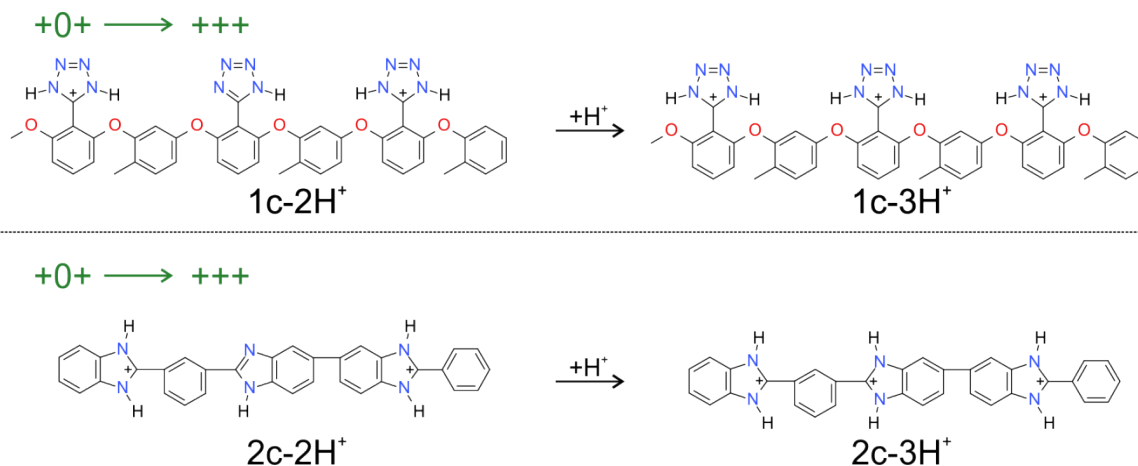

Figure S13. Structures/protonation reaction for systems considered in **Table S3**.

Effect of protonated-neighbouring units – neutral models (including PA species)

In the last step, the PA species were included in the models / reactions presented in **Figure S14** and **Table S4**.

Models **1c'**, **2c'** were constructed as follows:

    (i)   the polymer chain was fixed, i.e. the coordinates of the atoms in models presented in **Figure S13** were kept "frozen" ;

    (ii)   two phosphoric acid anions were added to the model, to partially compensate the positive charge of terminal units in previously considered models;

    (iii)   geometries of the PA⁻ anions were optimized (with fixed polymer chain)

For model **2c''** the additional three molecules of phosphoric acids were added and re-optimized.

The results presented in **Table S14** (for 1c', 2c') show again that the effect of the protonation of neighbouring units is much stronger for PBI than for TZPEEN. Now, the preference for the TZPEEN protonation is ca. 30 kcal/mol. Concerning the effect of additional PA molecules in **2c''** compared to **2c'**, the protonation energy is only slightly affected, going from -226 kcal/mol to -230 kcal/mol, and thus, not changing the qualitative picture.

However, it should be emphasized that the protonation of TZPEEN is likely overestimated in the models presented in **Table S4**, due to neglect of the chain relaxation, and due to the fact that the terminal trimer units are protonated. More complex, systematic studies, possibly based on larger models including more PA molecules, and considering many possible, alternative geometries, are needed to more quantitatively estimate the protonation energies. This is, however, beyond the scope of this manuscript and will be considered in future studies.

Table S4. The protonation energies for the central unit protonation in the systems with two protonated terminal units, interacting with two PA$^-$ anions (**1c'**, **2c'**), or five PA species (two PA$^-$ anions plus three neutral PA), **2c''**, ΔE_p,[1] in kcal/mol. The structures are shown in **Figure S14**.

Systems/protonation reactions:	ΔE_p[1]
1c': $\begin{array}{ccc} PA^- & PA^- & PA^- \\ + & 0 & + \end{array} \rightarrow \begin{array}{ccc} PA^- & PA^- \\ + & + & + \end{array}$ **1c'-2H$^+$** + H$^+$ → **1c'-3H$^+$**	-256.25 (-87.41)
2c': $\begin{array}{ccc} PA^- & PA^- & PA^- \\ + & 0 & + \end{array} \rightarrow \begin{array}{ccc} PA^- & PA^- \\ + & + & + \end{array}$ **2c'-2H$^+$** + H$^+$ → **2c'-3H$^+$**	-226.01 (-57.17)
2c'': $\begin{array}{ccc} PA^- & PA^- & PA^- & PA^- \\ + & 0 & + \\ PA & PA & PA \end{array} \rightarrow \begin{array}{ccc} + & 0 & + \\ PA & PA & PA \end{array}$ **2c''**+ H$^+$ → **2c''-3H$^+$**	-230.51 (-61.67)

[1] reaction energy for $XH_2^{2+}(H_2PO_4^-)_2$ + H$^+$ → $XH_3^{3+}(H_2PO_4^-)_2$ and for $XH_2^{2+}(H_2PO_4^-)_2$ + H_3O^+ → $XH_3^{3+}(H_2PO_4^-)_2$ + H_2O in brackets (for **1c'**,**2c'**), or correspondingly, the model including 5 PA species (for **2c''**)
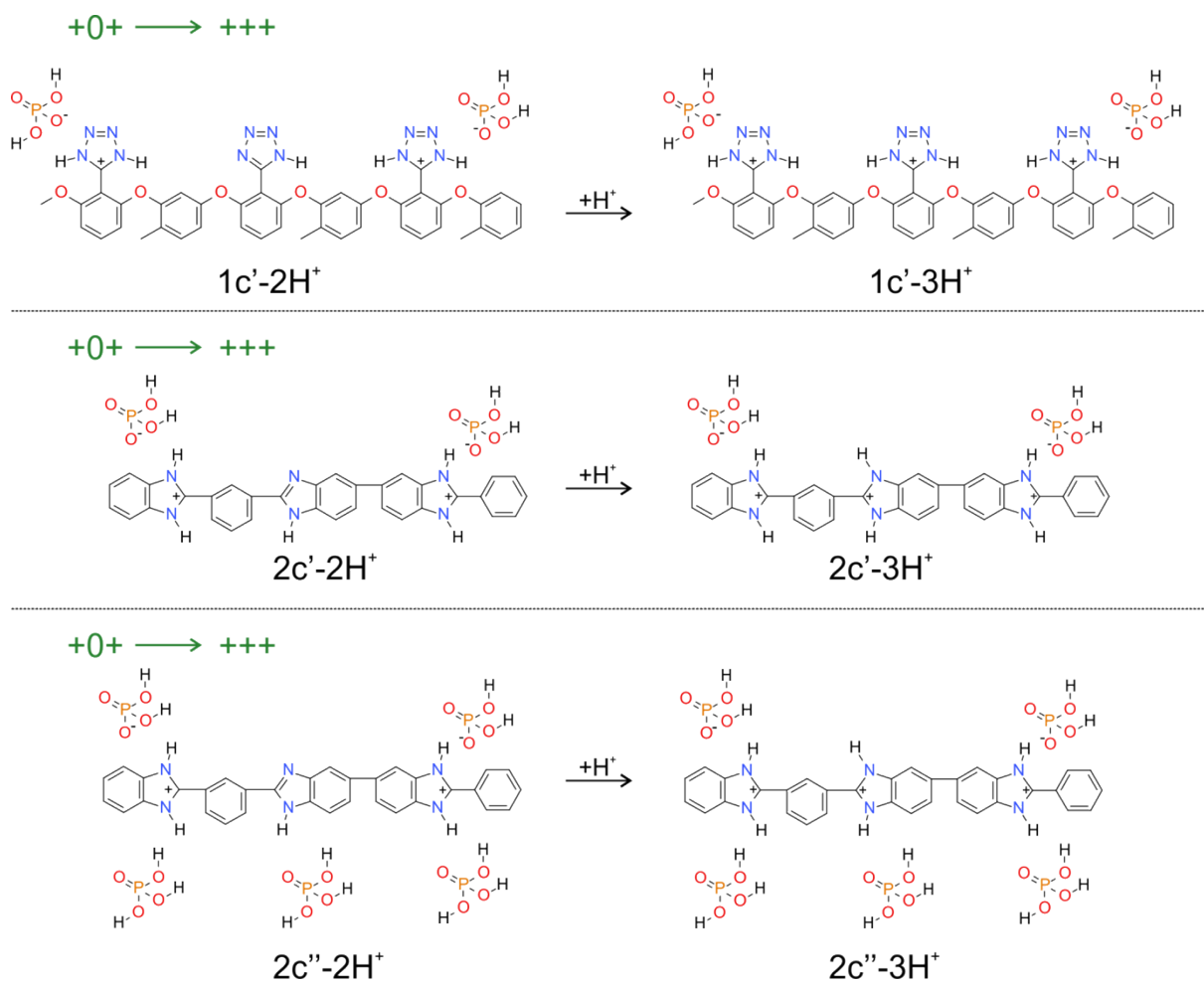

Figure S14. Structure/protonation reactions for systems considered in **Table S4**.